# Inverse Dynamics for Commanding Micromanipulator Inertial Forces to Damp Macromanipulator Vibration

Wayne J. Book
The G. W. Woodruff School of Mechanical Engineering
Georgia Institute of Technology
http://davinci.marc.gatech.edu – wayne.book@me.gatech.edu

Jeffery Cameron Loper
Lexmark International

## Introduction

For accurate positioning over a large workspace the use of a small (micro) manipulator mounted on the end of a large (macro) manipulator is an attractive configuration. However, the motion of the micromanipulator produces inertial forces on the end of the macromanipulator that serve as disturbances under normal decoupled control. Coupled control for rigid manipulators is possible but the high number of degrees of freedom (perhaps 9-12) creates a daunting task. If the macromanipulator is large and slender, as results from the weight and reach constraints of space, or the cross section and reach constraints of nuclear waste remediation applications, the macromanipulator will be significantly flexible. This can further complicate the control task. Book and Lee[1] proposed micromanipulator control that coordinated these inertial forces to damp macromanipulator vibration. That work and others by Lew et al.[2], Sharf[3], and Cannon et al.[4] struggled with providing robust, practically computable control that worked well for a wide range of macro and micro configurations. Demonstrations in special configurations for a limited number of degrees of vibrational freedom were encouraging, however. The current work largely overcomes these limitations. Desired micro-macro interaction forces are computed based on a simple damping algorithm. To determine the needed micromanipulator motions an inverse dynamics approach is used. The desired interaction forces can command either the necessary joint motion or joint torques as required for the current micro configuration. The concept has been implemented in laboratory experiments that illustrate the practical nature of the results.

## The Nature of the Problem and the Proposed Solution

Serial manipulators are typically fixed at one end (the proximal end) to a stationary or at least massive base. We want to position the other end precisely using the manipulator joints. Manipulators with distributed flexibility (e.g. flexible links and supporting structure) as well as manipulators with multiple points of lumped flexibility (e.g. flexible joints) may exhibit a nonminimum phase behavior that makes joint control extremely challenging. The collocation of actuators and output typically eliminates this condition. A rigid arm is effectively collocated. The macro/micromanipulator combination is noncollocated with respect to the macromanipulator actuators and its tip. The micromanipulator actuators are effectively collocated with the tip of the macromanipulator. Thus the generation of control forces in response to macro tip vibration is a minimum phase problem and more tractable.

One simple scheme for generating damping control forces that illustrates this effect is the dynamic vibration absorber. Figure 1 illustrates this concept in one degree of freedom if the force $F_s$ is produced by a spring and dashpot combination. Multi degree of freedom vibration absorbers also exist. Figure 1 can be implemented with all components being passive springs, masses and dampers. For flexible structure control of buildings and spacecraft engineers have implemented a related concept with active or semi-active control of a collection of one degree of freedom proof masses and reaction wheels that can provide inertial forces. If the sensors are collocated with actuators these controllers can imitate a passive controller and hence behave as would the passive system. The nature of the compliance and mass properties of the vibrating system can vary widely without affecting the conclusion that a dynamic vibration absorber is effective at reducing vibrations.

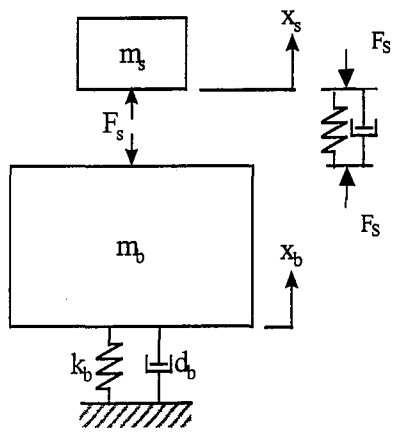


**Figure 1. Dynamic vibration absorber.**

Inspired by this simple and effective scheme for vibration damping we would like to control the micromanipulator to provide the necessary inertial reaction forces. Since the micromanipulator may have several degrees of freedom, inertial forces and moments

in several directions can be created, depending on the micromanipulator's configuration, velocities and actuator torques.

Practical issues and limitations should be addressed early in this discussion to not exaggerate what we might do. If the motion of the micromanipulator or the macro/micro combination are totally prescribed by the task, our approach is inadequate. In such a case we must continue to pursue the "holy grail" of complete coordinated joint control of this high order system. If we wish to position the tip of the macro arm this approach will help us and, depending on potential interference of the micro arm with objects in the workspace, can provide near ideal behavior. Also, if we are able to partition the task into rapid approach phases with the proposed damping scheme and more cautious capture phases this scheme can function well. This scheme can capitalize on the fact that vibrations, even of a relatively long macro arm, are of relatively high frequency compared to the motions we need to execute a task. One can capitalize on this separation of bandwidths (or time constants) with further techniques of singular perturbation analysis but that is not illustrated here. In such studies the range of travel required of the micromanipulator should also be examined for feasibility.

The **key contributions of this work** are to (1) show how to achieve the desired interaction forces between the micro and macromanipulators, (2) to simplify the resulting equations in a manner relevant to a specific realistic example, and (3) to verify the performance of this scheme on laboratory hardware.

## Overview of the Experimental System

While the approach used below appears to be quite general, some decisions and simplifications are made based on the experimental system available. It is appropriate to describe the experimental system at this time to provide the reader this background.

The test micromanipulator is the SAMII ( Small Articulated Manipulator II ) robot--a serial link, three degree-of-freedom robot found in the Intelligent Machine Dynamics Laboratory at Georgia Tech. The robot is attached to the end of a 20 foot aluminum beam, which is suspended from to an I-beam of the building. SAMII placed on the end of the beam allows for research into the control of macro/micromanipulator vibration, where SAMII is the micromanipulator and the beam acts as a macromanipulator. Figure 2 shows a photograph of this robot. Its first joint axis is along the axis of the supporting tube. Joints 2 and 3 are perpendicular to joint 1 and parallel to each other.

Controller calculations are executed on a *Motorola* 68060 processor board on a VME bus. The processor interfaces with a Digital to Analog converter board, an Analog to Digital converter board , and a Digital Input Output board, all also on the VME bus. *WindRiver* VxWorks, allows for C and C++ code and *Control Shell* implementation on the processor board.

The actuators of the system are hydraulic servo-motors at the joints of SAMII. These are double vane, and single vane actuators with electrohydraulic servo valves. The hydraulic actuators are single vane for joints one and three, and double vane for joint two. A pair of orthogonally placed quartz accelerometers measures acceleration of the beam tip. Optical encoders located on the shaft of each joint perform measurement of the rotational position of the joints

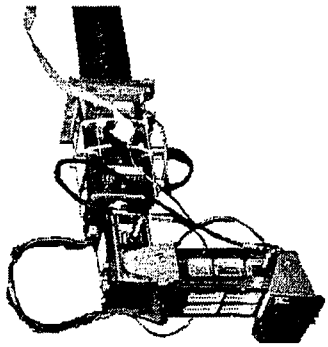

**Figure 2. The experimental micromanipulator SAMII shown mounted on the "macromanipulator" tube.**

## Dynamic Models

Dynamic models will be needed for the micromanipulator, the macromanipulator, and the actuators. Since we want to make explicit the interaction forces the Newton-Euler method is used to develop the equations for the micromanipulator. The primary purpose we have for the macro model is to justify some simplifications to our approach. That model is also useful for simulations in preparation for experiments, but limited space prevents us from discussing the simulations.

### Micromanipulator Model

The micromanipulator is a rigid arm but the base of the arm may be moving. Applying the standard Newton-Euler Algorithms to this situation the form of the inverse dynamic equations for the motion in joint coordinates is

$$\tau = B_\tau(\theta)\ddot{\theta} + N_{\tau,R}(\theta)[\dot{\theta}_i\dot{\theta}_j] + N_{\tau,N}(\theta)[\theta_i^2] + A_\tau(\theta)\alpha + G_\tau(\theta) \qquad (1)$$

where:

$\tau$ = the vector of joint torques and/or forces

$\theta$ = the vector of joint variables of the micromanipulator

B = a matrix of inertia-like terms

$N_{\tau,R}$ = a matrix of nonlinear functions of $\theta$ used in creating the Coriolis terms

$N_{\tau,N}$ = a matrix of nonlinear functions of θ used in creating the centrifugal terms
A = influence coefficients of the base accelerations
α = a vector of accelerations of the micromanipulator base
G = gravity contributions
$[\theta_i\theta_j]$ = vector of combinations of the joint variables for $i \neq j$
$[\theta_i^2]$ = vector of joint variables squared

For our implementation we need to expand these equations for the three axis arm which is pictured in Figure 2. The complete equations are detailed in Loper.[5]

We can also solve for the interaction forces produced by joint motion on the base of the micromanipulator. When a rigid robot is mounted on a rigid base these equations are usually unimportant unless one needs to design the base for strength. These equations are of the form

$$F_0 = B_F(\theta)\ddot{\theta} + N_{F,R}[\dot{\theta}_i\dot{\theta}_j] + N_{F,N}[\dot{\theta}_i^2] + A_F(\theta)\alpha + G_F(\theta) \quad (2)$$

The nomenclature is conveyed by the discussion for the previous equation, but the subscript is changed from τ to F to indicate the equations for $F_0$, the force on the base. Equations for reaction torque can be similarly derived.

## Macromanipulator Model

The "macromanipulator" involves only the unactuated flexible degrees of freedom. The important parameters of our "macro-manipulator" are:

- Length, L = 4.6482 m
- Diameter, d = 141.2875 mm
- Wall Thickness, t = 3.55 mm
- Cross Sectional Area, A = 7.77967e$^{-4}$ m$^2$
- Density, ρ = 2700 kg/m$^3$
- Mass, m = 9.7636 kg
- Modulus of Elasticity, E = 6.8948e$^{10}$ N/m$^2$
- Moment of Inertia, I = 684.479 kg-m$^2$

The compliance of the mounting "I" beam is significantly different in the two bending axes of the tube. Lagrangian techniques with two assumed modes in each of two perpendicular directions were used to derive a model for the beam. Bending moments and forces perpendicular to the beam axis are included. These inputs come from the micromanipulator reaction forces as derived above. The motions are well represented by linear second order differential equations, two degrees of freedom in the two directions as shown in equations below.

$$M_{Bx}\ddot{q}_x + D_{Bx}\dot{q}_x + K_{Bx}q_x = F_{IFx}$$
$$M_{By}\ddot{q}_y + D_{By}\dot{q}_y + K_{By}q_y = F_{IFy} \quad (3)$$

$q_x$ and $q_y$ are the modal state variables in x and y directions
$M_{Bx}$ and $M_{By}$ are the mass matrices in the x and y directions
$D_{Bx}$ and $D_{By}$ are the damping matrices to be determined experimentally
$K_{Bx}$ and $K_{By}$ are the modal spring constant matrices
$F_{IFx}$ and $F_{IFy}$ are the interaction forcing vectors.

For the experimental system we can derive the forcing vector $F_{IF}$. $F_x$ and $F_y$ are the interaction forces and $M_x$ and $M_y$ are the interaction moments collected into terms producing displacement in the x and y directions.

$$F_{IFx} = \begin{bmatrix} F_x(t) + 1.3576M_x(t)/L \\ F_x(t) + 4.4235M_x(t)/L \end{bmatrix}$$
$$F_{IFy} = \begin{bmatrix} F_y(t) + 1.3576M_y(t)/L \\ F_y(t) + 4.4235M_y(t)/L \end{bmatrix} \quad (4)$$

Analysis of the forcing terms shows the relative significance of torque and force in influencing the motion of the flexible vibrations. Force is much more significant factor in driving these equations partially due to the relatively large length L of the macromanipulator and the fact that moments and forces are of the same order of magnitude. This observation is supplemented with the following analysis showing that flexible rotation has minimal coupling to the torque on the micromanipulator base.

## Simplification Ignoring Flexible Rotation

The complexity experienced in including rotation of the micro's base due to flexibility of the macro led us to consider the relative significance in terms using a simplified analysis. A simple lumped model for the coupled macro/micro model was used. One passive joint at the base of the macro represented flexibility with a lumped spring $K_\theta$ about the assumed passive joint rotation $\theta_1$. The micromanipulator was represented as a single joint with angle $\phi_2$ about which torque $\tau_2$ is applied. Realistic values for the inertias ($I_{zz,1}$ and $I_{zz,2}$) can be assumed to make this a representative model.

$$\tau_A = I_{zz,1}\ddot{\theta}_1 + I_{zz,2}(\ddot{\theta}_1 + \ddot{\theta}_2) - K_\theta\theta_1 + m_1 g r_{c,1}\sin(\theta_1) + m_2 g r_{c,2}\sin(\theta_1 + \theta_2) \quad (5)$$

$$\tau_B = I_{zz,1}\ddot{\theta}_1 + I_{zz,2}\ddot{\theta}_2 - K_\theta\theta_1 + m_1 g r_{c,1}\sin(\theta_1) + m_2 g r_{c,2}\sin(\theta_2) \quad (6)$$

The equation (5) for $\tau_A$ represent the combined model while the equation (6) for $\tau_B$ represents the model without including flexible rotation. The differences were due to gravity potential energy change due to $\theta_1$, extremely small, and the differences in total angular acceleration compared to the acceleration using $\theta_2$ alone. Based on the difference in relative rotations the error in ignoring

flexible rotation on the micro arm was approximately 1/100. This justified the simplification for the experiments described below.

## Combined Model

As developed above we have equations for base forces (7) and equations for joint torques (8)

$$F = B_F(\theta)\ddot{\theta} + N_F(\dot{\theta},\theta,\alpha) \qquad (7)$$

$$\tau = B_\tau(\theta)\ddot{\theta} + N_\tau(\dot{\theta},\theta,\alpha) \qquad (8)$$

Solving the second of these equations for joint acceleration and substituting into the first equation we find the force at the base of the micromanipulator in terms of joint torques is

$$F = B_F B_\tau^{-1}(\theta)[\tau - N_\tau(\dot{\theta},\theta,\alpha)] + N_F(\dot{\theta},\theta,\alpha) \qquad (9)$$

Depending if we can specify the angular acceleration or the torque of the joints we use one or the other of the previous two equations. In our experiments we can approximately command the joint torque so we solve for that given the desired interaction force and actual joint position and velocity as shown in (10).

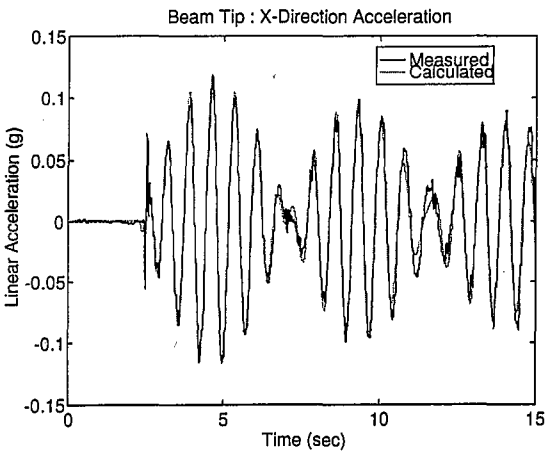


**Figure 3. Example of Correspondence between Predicted and Measured Acceleration. (Joint 2 in motion)**

$$\tau = B_\tau B_F^{-1}(\theta)[F - N_F(\dot{\theta},\theta,\alpha)] + N_\tau(\dot{\theta},\theta,\alpha) \qquad (10)$$

## Experimental Verification of Model

Verification experiments employed :sinusoidal inputs of 1.3 Hz to joint 2 of the micromanipulator with joints 1 and 3 fixed and to joint 1 of the micromanipulator with joints 2 and 3 fixed. Accelerations were measured in orthogonal directions and compared to simulations. Figure 3 illustrates the typical correspondence of the data which was considered very good.

## *The Control Algorithm*

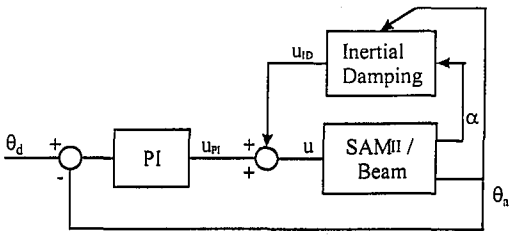


**Figure 4. Overall control block diagram.**

### Joint Control

Joint reference values are compared to measured values.to create an error signal that is entered into a PI control algorithm. Each joint is designed independently for our experimental system. Since the hydraulic motors are quite strong there is little disturbance of the joint angle experienced as a result of the actuation of other joints or the motion of the base. The transfer function of the hydraulic actuator is approximated as a first order time constant $k_2$ plus integrator. The choice of P and I gains was carried out with root locus analysis for acceptable joint control response. The details are fairly standard but are found in the thesis by Loper.[5]

## Damping Control

$$\frac{F_s}{x_b} = s^2(b_s m_s s + k_s m_s) \qquad (11)$$

The inertial damping of the dynamic vibration absorber (Figure 1) was the original inspiration for this control approach. The transform interaction forces between the large and small mass can be obtained from a simple modeling exercise and is given in (11).

The nomenclature is obvious from Figure 1 except that s is the complex Laplace variable.

## Acceleration Feedback

To perfectly reproduce this behavior with a hydraulic or other actuator of the micromanipulator would require some additional computation from the measured (via accelerometers in our experiment) macromanipulator vibration motion. We chose to consider a simpler alternative complimentary to our actuators.

The actuator transfer function must be included in the effect of feedback. Using the measurement of

acceleration of the base multiplied by an acceleration gain $k_a$ as an input to the hydraulic actuator produces the following interaction force as related to base position

$$\frac{F_s}{x_b} = s^2\left[\frac{(k_1k_a + k_2)m_s s + m_s}{k_2 s + 1}\right] \qquad (12)$$

Comparison of this transfer function to the transfer function for the passive dynamic vibration absorber reveals similar response if $k_2$, the hydraulic time constant, is small. The gain $k_a$ allows adjustment of the damper term of the equation but the spring equation cannot be adjusted for best performance. The compromise was accepted for the sake of simplicity in view of the relatively good performance using only acceleration feedback.

To evaluate the response of acceleration feedback on our experimental system, root locus analysis for the actuation in orthogonal directions was performed. The experimentally determined value of $k_2 = 0.05$ was used and average values of the micromanipulator inertia was used. The result for axis two was very similar. We show the x direction, which is the direction with the lower spring constant for the mounting of the macromanipulator. The root locus in Figure 5 shows the lightly damped vibration poles are moved to the left in the complex plane by increasing $k_a$. Note that natural frequency begins to decrease as $k_a$ is increased above a value of about 200.

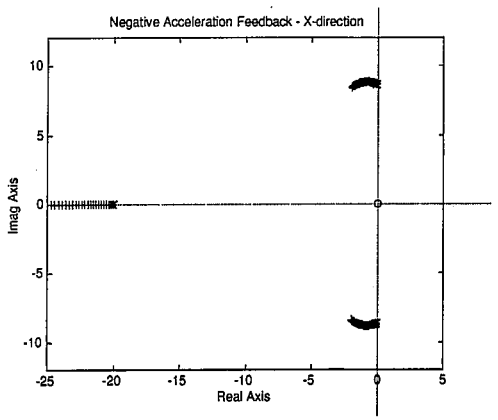


**Figure 5. Predicted result for varying acceleration feedback $k_a$.**

### Inverse Dynamics Transformation

The micromanipulator needs to generate forces to provide the results predicted above. The forces to be generated at the base of the micromanipulator are commanded by the accelerometer measurements. The movements that will produce the forces can be computed from the dynamics equations in the nontraditional form of equations (7) and (8).

In a more general case the number of micro joints are equal to n. For our experiments n=3. For $n \geq 6$ one might hope to totally prescribe all forces and moments on the base. Our modeling of the combined arm has revealed that the influence of forces perpendicular to the tube axis of the "macromanipulator" is much greater on the dominant vibrational modes. Consequently, we have adequate dimensions, and in fact rely on only the first two joints of the micromanipulator since they move larger link masses and hence are more effective at generating forces. In general an analysis to resolve this case of over actuation or redundancy might be appropriate.

We have solved for the general case above in equation (10). While the current command to the electro-hydraulic valves does not produce a simple torque output from the actuators, that assumption provides a useful insight. When we are primarily damping vibration, the joints of the micromanipulator are moving back and forth to generate oscillating forces at approximately the frequency of the macromanipulator vibration. At this relatively high frequency the resulting velocity remains small. Hence the centrifugal and Coriolis forces remain small and can be ignored in equation (10). Combining the acceleration feedback with the dynamics under these circumstances yields (13).

$$\tau = B_\tau B_F^{-1}(\theta)K_a\alpha. \qquad (13)$$

For our experiments only two elements of torque $\tau$ and acceleration $\alpha$ were used, and the matrix $K_\alpha$ was based on the root locus plot further refined by tuning.

## *Experimental Results*

The concepts described require experimental validation to warrant further consideration. The experimental system described above provides a realistic test bed for these experiments in that

(a) multiple degrees of freedom are involved with significant nonlinearities in the dynamics,
(b) realistic actuators are used to implement the micromanipulator,
(c) the sensors used are practical for implementation on a wide range of problems, although filtering or compensation might be necessary if the accelerometers are aligned with gravity
(d) the computational hardware is representative of that available for practical implementation.

The experiments do not include actual motion of the "macromanipulator." This significant simplification in constructing a test bed enabled testing here, but further experiments would clearly be of interest.

### Response to Disturbances

The beam has two decoupled modes of vibration dependent upon the boundary conditions imposed by the supporting I-beam. These two modes have different fundamental frequencies, which were experimentally measured at 11.84 rad/s for the *Y*-direction (parallel to the supporting I-beam) and 9.06 rad/s for the *X*-direction (perpendicular to the supporting I-beam). The outcome of the beam having these two independent vibration

responses means that the controller as well gives two different sets of responses with the inertial damping. Ultimately the controller works faster for the higher frequency direction because of the fact that it responds proportional to the measured acceleration of the beam, which in this case would be faster. The controller primarily lets joint two respond to vibration in the direction of links two and three, which then allows joint one to handle other vibration. When both of the decoupled modes of vibration are actuated then the controller response of joints one and two becomes quite complex, but they never interfere with each other.

Several experiments were performed to test the effectiveness of the controller under different circumstances. The configurations of each experiment, the direction of applied disturbances are presented in Table 1. The joints used by the controller are also listed.

The full controller uses both joints one and two for actuation, but it is interesting to note that either joint alone is sufficient in decreasing the settling time for most configurations. Experiment 3 shows this effect, where the configuration of the robot places the links between the *X* and *Y*-direction. For this experiment disturbances are applied to both of these directions but are unequal such that the motion is not in phase.

As a measure of the performance of the controller damping ratios of the response are measured after the controller is activated. These damping ratios are tabulated in Table 2 and should be compared to the freely vibrating system that had a damping ratio of .0059 in the x direction and .0019 in the y direction.

**Table 1. Experiment Parameters.**

| No. | $\theta_1$ (rad) | $\theta_2$ (rad) | Joints Actuated | Applied Disturbance |
|---|---|---|---|---|
| **1.a** | 0 | $\pi/4$ | 1 | Y |
| **1.b** | $-\pi/2$ | $\pi/4$ | 1 | X |
| **2.a** | 0 | $\pi/4$ | 2 | X |
| **2.b** | $-\pi/2$ | $\pi/4$ | 2 | Y |
| **3** | $-\pi/4$ | $\pi/4$ | 1 & 2 | X & Y |

**Table 2. Experiment results (damping ratios).**

| No. | Damp ratio X | Damp ratio Y | Times better X | Times Better Y |
|---|---|---|---|---|
| **1.a** | ~~ | 0.195 | ~~ | 102 |
| **1.b** | 0.107 | ~~ | 18 | ~~ |
| **2.a** | 0.151 | ~~ | 26 | ~~ |
| **2.b** | ~~ | 0.363 | ~~ | 191 |
| **3** | 0.198 | 0.158 | 34 | 83 |

For experiment 1.a the beam at first is freely vibrating to a disturbance in the *Y*-direction and then at some arbitrary time the controller is turned on. The controller in this case only uses the first joint for actuation. Physically this means that the robot is lying in the *X*-direction but responds to disturbances perpendicular to it. Once the controller is turned on, it is seen that the beam settles quickly within two seconds. Similar results are seen for experiment 1.b, except the directions are reversed because the arms lie in the *Y*-direction. The settling times as seen by comparing 1.a and 1.b are longer for *X*-direction accelerations, which is explained by the fact that the natural frequency of the beam is smaller in that direction. That means it takes longer to actuate in response to the slower accelerations

Experiments 2.a and 2.b use joint two only to actuate in response to acceleration. A Comparison of experiments 1 and 2 shows that the settling times are relatively similar and that neither is superior to the other. In the full controller though both joints one and two are used to actuate.

Experiment 3 shows the total controller responses. The configuration places links two and three between both axis and disturbances are applied in both directions. The settling times decrease for the *X*-axis acceleration to approximately 2 seconds and 1.5 seconds for *Y*-axis acceleration. The time history of the macro tip acceleration and the position of the joints is plotted in Figure 9. Note that the joints remain essentially stationary until the damping controller is turned on.

What can be deduced from the results is that the total controller is faster than either separate controller of experiments 1 and 2. When the configuration of the robot over its workspace is considered the total controller is much better suited. This fact arises because sometimes single joint actuation alone cannot achieve the damping forces necessary.

## Response to Commanded Micromanipulator Joint Motion

To analyze the effectiveness of the controller during motion a step response is supplied to each joint simultaneously. The step response takes joint one from 0 to $-\pi$ radians and joint two from 0.5 to 1 radians. Both the free response and that with the inertial damping are shown in Figure 10. For the *X*-direction acceleration the controller takes approximately 4 seconds to settle the vibration. As noted earlier the controller works better in general in the *Y*-axis because the frequency of vibration is higher and therefore the period of oscillations is smaller. This is true for the step responses, with a settling time of only 2 seconds. The important conclusion to draw from this experiment is that the controller uses the actuation of both joints in a collaborative method. It should also be recognized that step commands are not typically given to joints in application, but this test command is readily implemented and explained to convey the performance of the controller.

## Conclusions

A multi degree of freedom manipulator can be commanded to generate base forces by utilization of the dynamic equations relating joint torques or joint accelerations to base forces. This can be extended to a full order case with three base moments and three base forces. In the experiments described two forces were sufficient to damp the fundamental modes. With a force command capability a variety of damping algorithms can be used to determine the desired force. A simple acceleration feedback algorithm was used here which approximates a two degree of freedom dynamic vibration absorber where the damping coefficient can be adjusted by the acceleration feedback gain. The resulting damping ratio of the fundamental mode was increased by factors of between 18 and 191.

The ability to generate active damping forces and moments at the point of interest results in collocated control. We have shown that with justifiable simplifications the resulting controller is effective, robust and requires a modest amount of calculation.

Further development of this concept is appropriate in light of its effectiveness and the need to adapt the controller to macromanipulator motion, which was not treated here.


### Acknowledgements

This work was partially sponsored by DOE Contract AK-9037 and by support from NEC Corporation.


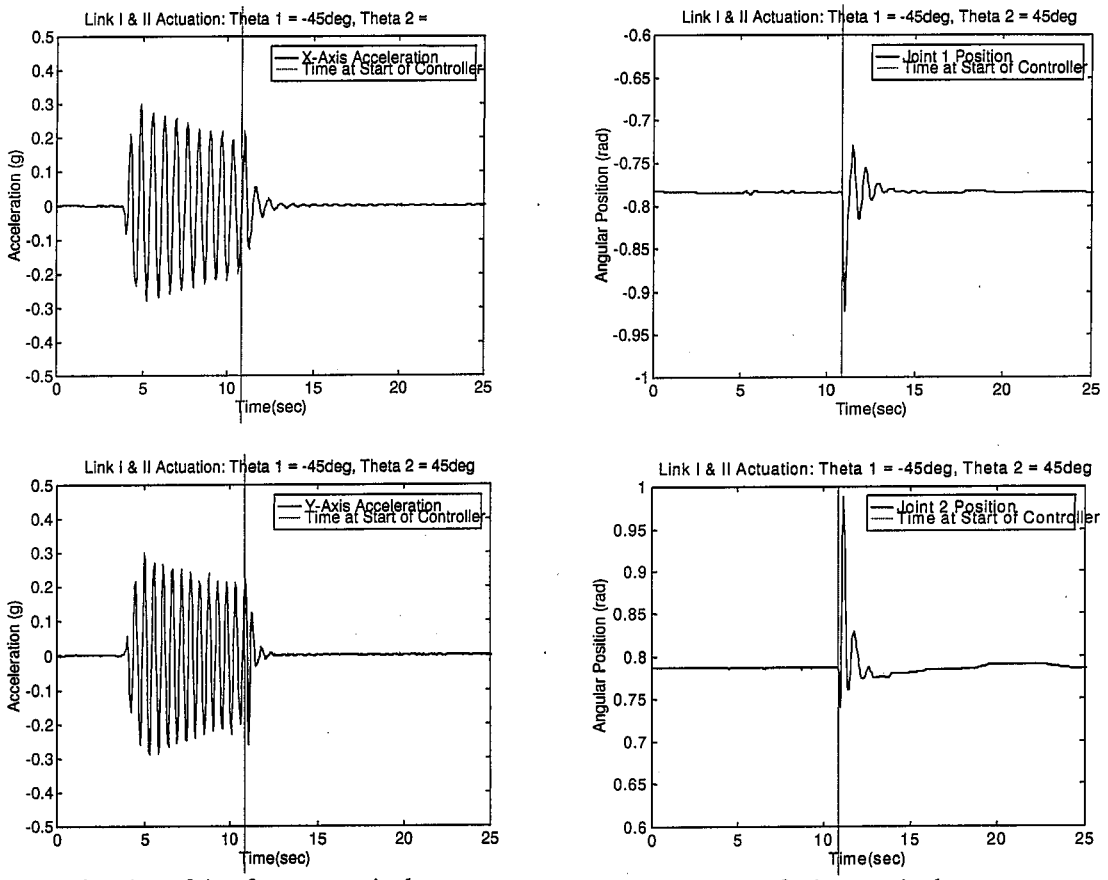


(a) Acceleration of tip of macromanipulator

(b) Joint motion of micromanipulator

**Figure 9. Response to a disturbance of the macromanipulator.**

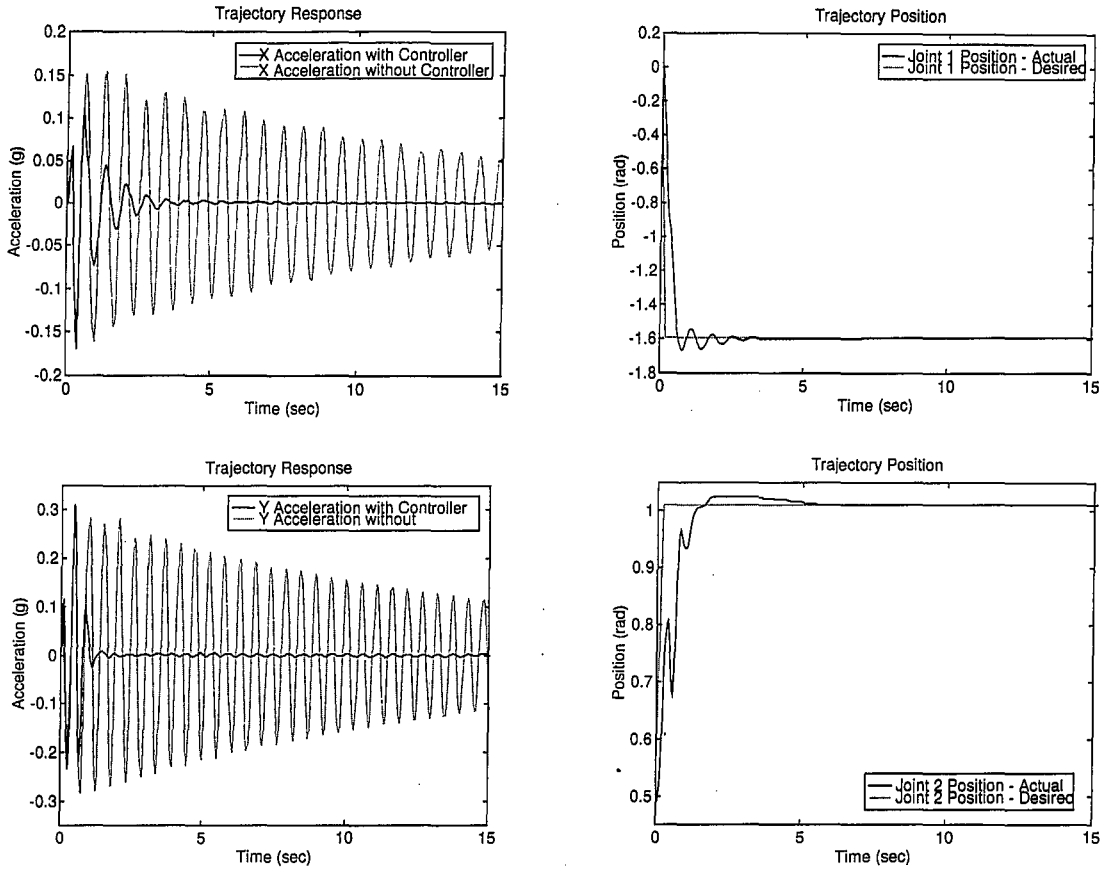


(a) Acceleration of macromanipulator for commanded micromanipulator motion.

(b) Joint motion in response to a step command.

**Figure 10. Response to a step command to the micromanipulator.**

## References


[1] Book, W. and S.-H. Lee, "Vibration Control of a Large Flexible Manipulator by a Small Robotic Arm," ***Proceedings of the American Control Conference***, Vol. 2, pp. 1377-1380, 1989.

[2] Lew, J., D. Trudnowski, and D. Bennett, "Micro Manipulator Motion Control to Suppress Macro Manipulator Structural Vibration" ***Proceedings – IEEE International Conference on Robotics and Automation***, Vol. 2, pp. 3116-3120, 1995.

[3] Sharf, I., "Active Damping of a Large Flexible Manipulator with a Short-Reach Robot," ***Proceedings of the American Control Conference***, Vol. 5, pp. 3329-3333, 1995.

[4] Cannon, D., P. Magee, W. Book, and J. Lew, "Experimental Study on Micro/Macro Manipulator Control," ***Proceedings – IEEE International Conference on Robotics and Automation***, Vol. 3, pp. 2549-2554, 1996.

[5] Loper, J.C., "Vibration Cancellation and Disturbance Rejection in Serially Linked Micro/Macro Manipulators," M.S. Thesis, Georgia Institute of Technology, School of Mechanical Engineering, March 1998.